

Unitary Gas Constraints on Nuclear Symmetry Energy

Evgeni E. Kolomeitsev,^{1,*} James M. Lattimer,^{2,†} Akira Ohnishi,^{3,‡} and Ingo Tews^{4,§}

¹Faculty of Natural Sciences, Matej Bel University, Tajovskeho 40, SK-97401 Banská Bystrica, Slovakia

²Department of Physics & Astronomy, Stony Brook University, Stony Brook, NY 11733

³Yukawa Institute for Theoretical Physics, Kyoto University, Kyoto 606-8502, Japan

⁴Institute for Nuclear Theory, University of Washington, Seattle, WA 98195-1550

(Dated: July 8, 2022)

We show the existence of a lower bound on the volume symmetry energy parameter S_0 from unitary gas considerations. We further demonstrate that values of S_0 above this minimum imply upper and lower bounds on the symmetry energy parameter L describing its lowest-order density dependence. The bounds are found to be consistent with both recent calculations of the energies of pure neutron matter and constraints from nuclear experiments. These results are significant because many equations of state in active use for simulations of nuclear structure, heavy ion collisions, supernovae, neutron star mergers, and neutron star structure violate these constraints.

The nuclear symmetry energy is one of the decisive ingredients in compact star astrophysics as well as in nuclear physics. It provides the pressure of neutron star matter, which is nearly pure neutron matter (PNM) near the saturation density $n_0 \simeq 0.16 \text{ fm}^{-3}$, which largely determines neutron star radii [1] and therefore properties of their crusts, moments of inertia, tidal polarizabilities and binding energies [2]. The symmetry energy is also important in calculations of the r-process [3], supernovae [4], and neutron star mergers [5]. Terrestrial experiments measuring nuclear masses, dipole resonances and neutron skin thicknesses can constrain the symmetry energy [6], as can experiments using normal and radioactive nuclear beams [7].

A possible source of additional information is the unitary gas. Universal behavior emerges for fermions interacting via pairwise s -wave interactions with an infinite scattering length (a_0) and a vanishing effective range (r_{eff}), *i.e.* the unitary gas (see Ref. [8] for an historical review). Since in this case the average particle distance is the only length scale of the system, the ground state energy per particle in the unitary gas E_{UG} is proportional to the Fermi energy E_{F} , $E_{\text{UG}} = \frac{3}{5} E_{\text{F}} \xi$, where ξ is referred to as the Bertsch parameter and has the experimentally measured value $\xi \simeq 0.37$ [9, 10]. PNM at low densities is considered to be close to the unitary limit since the s -wave scattering length of the nn system is $a_0 = -18.9 \text{ fm}$. This corresponds to $(a_0 k_{\text{F}})^{-1} \simeq -0.03$ at n_0 , where $k_{\text{F}} = (3\pi^2 n)^{1/3}$ is the neutron Fermi momentum, whereas the unitary gas limit is $(a_0 k_{\text{F}})^{-1} = 0$.

We demonstrate that nuclear symmetry energy parameters are significantly constrained by the unitary gas energy, based on the conjecture that E_{UG} provides the lower bound of the energy per nucleon in PNM (E_{PNM}),

$$E_{\text{PNM}}(n) \geq E_{\text{UG}}(n). \quad (1)$$

Justification of the conjecture: For spin-one-half fermions interacting solely via the s -wave interactions without two-body bound states ($a_0 < 0$), the unitary limit, $a_0 \rightarrow -\infty$ and $r_{\text{eff}} \rightarrow 0$, indicates the largest attraction. Thus, the unitary gas energy should serve as a lower bound for E_{PNM} at low densities. At higher densities, however, p and higher par-

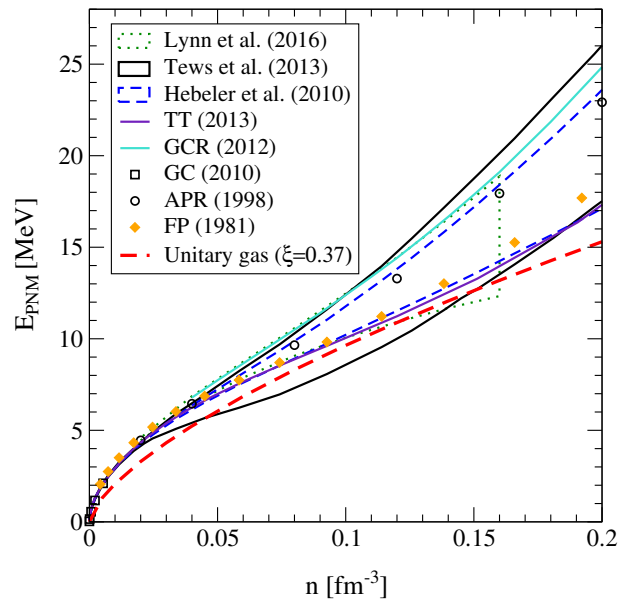


FIG. 1. Unitary gas bound with $\xi = 0.37$ compared to ab initio calculations of Refs. [12] (Lynn et al.), [11] (Tews et al.), [13] (Hebeler et al.), [14] (TT), [15] (GCR), [16] (GC), [17] (APR), [18] (FP).

tial wave interactions may spoil this bound. For example, the average p -wave interaction is very small but attractive.

When comparing the unitary gas with calculations using only nucleon-nucleon (NN) interactions, one finds that neutron matter behaves approximately as a unitary gas. Softer NN interactions lead to slightly more attraction compared to the unitary gas and harder interactions give slightly more repulsion. This may be due to less short-range correlations for softer interactions. In the NN-only results of Ref. [11], the maximum difference of the energy from that of the unitary gas is approximately 2 MeV at n_0 .

In neutron matter, however, recent ab initio calculations showed the importance of the inclusion of three-body (3N) forces, which are repulsive in low- to moderate-density neutron matter and increase the neutron-matter energy by several MeV at n_0 . In Fig. 1 we show a comparison of the unitary gas

bound with several ab initio calculations for PNM including both NN and 3N forces of Refs. [11–18]. Only two calculations intersect with the unitary gas constraint within their uncertainty bands and for the softest interactions: a chiral N³LO calculation [11] and Quantum Monte Carlo N²LO calculations using chiral forces [12]. For the first this is due to the behavior of one particular Hamiltonian at intermediate densities, while for the latter this is due to the use of local regulators, which lead to less repulsion from 3N forces [19].

Thus, empirically one finds $E_{\text{PNM}} > E_{\text{UG}}$ in ab initio calculations. Although it cannot be proven that the unitary gas is a lower bound for the neutron matter energy at all densities, the combination of effective-range effects, small tensor interactions, and repulsive 3N forces in neutron matter strongly suggests that this conjecture is justified.

Constraint on symmetry energy: At baryon density $n = u n_0$, the unitary gas energy is given as

$$E_{\text{UG}}(u) = \frac{3}{5} E_{\text{F}}(n) \xi = \frac{3\hbar^2 k_{\text{F}}^2}{10m_n} \xi = E_{\text{UG}}^0 u^{2/3}, \quad (2)$$

where m_n is the neutron mass and $E_{\text{UG}}^0 = E_{\text{UG}}(u=1)$. Symmetric nuclear matter energy (E_{SNM}) can be expanded as

$$E_{\text{SNM}}(u) = E_0 + K(u-1)^2/18 + \mathcal{O}[(u-1)^3], \quad (3)$$

where $E_0 \simeq -16$ MeV and $K \simeq 230$ MeV are the saturation energy and incompressibility parameters, respectively. We define the symmetry energy as $S(u) = E_{\text{PNM}}(u) - E_{\text{SNM}}(u)$. The conjecture (1) yields the lower bound $S^{\text{LB}}(u)$:

$$S(u) \geq E_{\text{UG}}^0 u^{2/3} - \left[E_0 + \frac{K}{18} (u-1)^2 \right] \equiv S^{\text{LB}}(u). \quad (4)$$

In Fig. 2, we show the lower bound on $S(u)$ imposed by the unitary gas using typical values for the nuclear parameters. The shaded area shows the excluded region, inside which $S(u)$ should not enter. From Eq. (4), it is clear that $S_0 \equiv S(u=1)$ is bounded from below, $S_0 \geq E_{\text{UG}}^0 - E_0 \equiv S_0^{\text{LB}}$. At $S_0 = S_0^{\text{LB}}$, the slopes of $S(u)$ and $S^{\text{LB}}(u)$ must agree as shown by the dashed line in Fig. 2, and we thus find

$$L \equiv 3 dS^{\text{LB}}/du|_{u=1} = 2E_{\text{UG}}^0 \equiv L_0, \quad (5)$$

These values are independent of K , the most uncertain of the saturation parameters, and thus appear to be very general.

For a given value of $S_0 > S_0^{\text{LB}}$, L takes the upper (or lower) bound when $S(u)$ becomes tangent to the region excluded by $S^{\text{LB}}(u)$, as shown by solid lines in Fig. 2. Calculation of the tangent conditions requires some assumptions about the functional form of $S(u)$.

It is often assumed that the nuclear energy $E(u, x)$, where x is the proton fraction, can be quadratically interpolated between E_{SNM} and E_{PNM} , i.e., $E(u, x) \simeq E(u, 1/2) + S(u)(1-2x)^2$ with no higher order terms. Recent calculations of neutron-rich matter [20] have, in fact, shown that this is highly accurate at all densities, for both $x \simeq 1/2$ and

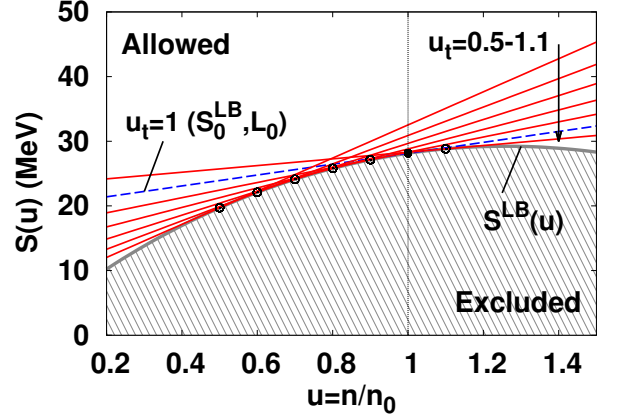


FIG. 2. Unitary gas bound on the symmetry energy, using Eq. (4) and parameters in Eq. (9). Hatched area shows the excluded region of $S(u)$. Solid lines show those cases where $S(u)$ becomes tangent to the boundary.

$x \ll 1/2$. Then one can Taylor expand $S(u)$ around $u = 1$ using the usual symmetry parameters S_0 , L , and K_{sym} ,

$$S(u) = S_0 + \frac{L}{3} (u-1) + \frac{K_{\text{sym}}}{18} (u-1)^2 + \mathcal{O}[(u-1)^3]. \quad (6)$$

This allows Eq. (4) to be expressed as

$$S_0 + \frac{L}{3} (u-1) \geq E_{\text{UG}}^0 u^{2/3} - \left[E_0 + \frac{K_n}{18} (u-1)^2 \right], \quad (7)$$

where $K_n = K + K_{\text{sym}}$ is the incompressibility of PNM. The condition that both $S = S^{\text{LB}}$ and $dS/du = dS^{\text{LB}}/du$ at the tangent density u_t leads to the parametric equations

$$\begin{aligned} S_0 &= \frac{E_{\text{UG}}^0}{3u_t^{1/3}} (u_t + 2) + \frac{K_n}{18} (u_t - 1)^2 - E_0, \\ L &= \frac{2E_{\text{UG}}^0}{u_t^{1/3}} - \frac{K_n}{3} (u_t - 1). \end{aligned} \quad (8)$$

For every value of u_t , one can then determine a point on the boundary of the excluded region, i.e., $S_0(L)$. By expanding $E_{\text{UG}}(u)$ around $u = 1$ to the second order, we can obtain an approximate but analytic form of this boundary as $S_0 = E_{\text{UG}}^0 - E_0 + (L - 2E_{\text{UG}}^0)^2 / [2(2E_{\text{UG}}^0 + K_n)]$.

The (S_0, L) boundary depends on the saturation and unitary gas parameters, $n_0, E_0, K, K_{\text{sym}}$ and ξ , and becomes less exclusionary the smaller $E_{\text{UG}}^0 \propto n_0^{2/3} \xi$, or the larger E_0 and K_n , are chosen. The experimental values of the saturation properties are $E_0 = -15.9 \pm 0.4$ MeV, $n_0 = 0.164 \pm 0.007$ fm⁻³ [21], and $K = 240 \pm 20$ MeV [22, 23] or $K = 230 \pm 40$ MeV [24]. In general, $K_{\text{sym}} < 0$ for realistic relativistic mean field and Skyrme forces, i.e., those that have been fit to properties of laboratory nuclei. For example, N³LO chiral EFT calculations [11] yield $K_n = 119 \pm 101$ MeV [25]. Therefore, using $K_n = K$ is a conservative choice. The Bertsch parameter for spin-half fermions

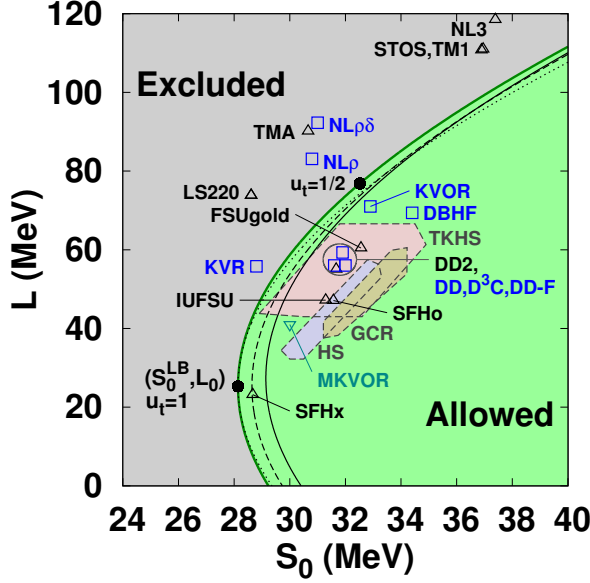


FIG. 3. Unitary gas bound on the symmetry energy parameters from Eq. (8) using the conservative parameter set from Eq. (9) is shown as the thick solid curve. The colored region to the left of this curve is excluded. Filled circles show the points at the tangent density $u_t = 1$, where $(S_0, L) = (S_0^{LB}, L_0)$, and $u_t = 1/2$. Alternative bounds from variations of parameters are shown as thin solid ($\delta E_{UG}^0 = +1.0$ MeV), dotted ($\delta K_n = -30$ MeV) and dashed ($\delta E_0 = -0.5$ MeV) curves. Values for interactions used in tabulated equations of state for astrophysical simulations are shown as triangles (notation and data from Ref. [4]). We also show values of other frequently used interactions as open squares (from Ref. [26]) and the inverted triangle (from Ref. [27]). Parameter ranges inferred from PNM calculations of Refs. [11, 13, 15] are shown as the shaded regions TKHS, GCR and HS, respectively.

is experimentally measured to be $\xi = 0.376 \pm 0.004$ [9] or $\xi = 0.370 \pm 0.005 \pm 0.008$ [10]. Thus we adopt

$$\begin{aligned} E_0 &= -15.5 \text{ MeV}, \quad n_0 = 0.157 \text{ fm}^{-3}, \\ K &= 270 \text{ MeV}, \quad K_{\text{sym}} = 0, \quad \xi = 0.365, \end{aligned} \quad (9)$$

as a conservative parameter set. We find $E_{UG}^0 = 12.64$ MeV, $S_0^{LB} = 28.14$ MeV, and $L_0 = 25.28$ MeV.

In Fig. 3, the thick solid curve shows the resulting bound on S_0 and L from the unitary gas constraint. The point where $u_t = 1/2$ is indicated, where $L \simeq 77$ MeV, showing a plausible limit of applicability of Eq. (6); note that this relation predicts $S(0) = S_0 - L/3 + K_{\text{sym}}/18$ while $S(u)$ should, in fact, vanish for $u \rightarrow 0$. Eq. (8) shows that $L = 0$ MeV when $u_t = 1.265$, in which case Eq. (6) is still reliable. This figure also shows how varying assumptions about the saturation and unitary parameters changes the bound. Note that only variations in E_0 , K_n and E_{UG}^0 need be considered.

To demonstrate the significance of the unitary gas bound, we have plotted in Fig. 3 the values of the symmetry energy parameters used in ten tabularized equations of state frequently used [4] for astrophysical simulations. Note that half

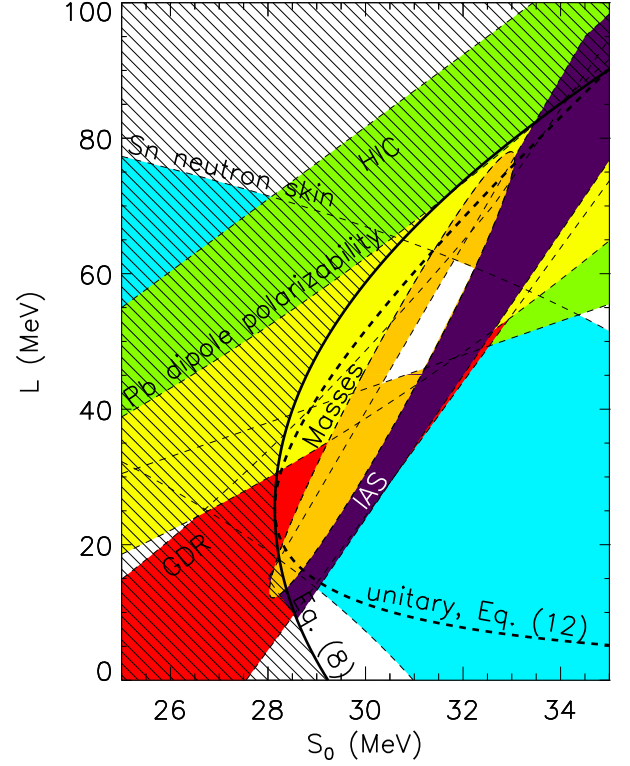


FIG. 4. Unitary gas bounds on symmetry energy parameters compared with experimental constraints taken from Ref. [6, 30]. The thick black solid curve shows the bound from Eq. (8) and the parameter set in Eq. (9). The thick black dashed curve shows the bound from Eq. (12) and the same parameter set except that K_{sym} is determined from Eq. (10) using $\alpha = 3$ and $\beta = K$.

of them violate the bound, which demonstrates the need for additional equation of state tables that satisfy these minimal constraints. We also show the results of other commonly used interactions [26, 27], among which a non-trivial number of interactions are found to violate the bound.

It is interesting to note that realistic forces, of both non-relativistic potential and relativistic field theoretical types, predict a reasonably tight correlation between K_{sym} and L that is, approximately, [28, 29]

$$K_{\text{sym}} \simeq \alpha L - \beta, \quad (10)$$

where $\alpha \sim 3$ and $\beta \sim 270$ MeV. The coincidence that β is close to our upper limit to K implies $K_n \simeq 3L$, and allows the boundary (8) to be expressed as

$$S_0 = \frac{E_{UG}^0}{3} \frac{1 + 2u_t^2}{u_t^{4/3}} - E_0, \quad L = \frac{2E_{UG}^0}{u_t^{4/3}}, \quad (11)$$

or, eliminating u_t , simply as

$$S_0 = \frac{L}{6} \left[1 + 2 \left(\frac{2E_{UG}^0}{L} \right)^{3/2} \right] - E_0. \quad (12)$$

The two forms for the exclusion boundary are compared in Fig. 4. We note that the two bounds cross when $L = K/3$, and that $L \geq 0$ in the latter form.

Comparison with experimental constraints: Experimental constraints on symmetry energy parameters are reviewed in Refs. [6] and [7]. They indicate that consistency with measurements of nuclear masses, giant dipole resonances and dipole polarizabilities, neutron skin thicknesses, isobaric analog states and flows in heavy ion collisions is achieved for $30 \text{ MeV} \leq S_0 \leq 32 \text{ MeV}$ and $40 \text{ MeV} \leq L \leq 60 \text{ MeV}$ (Fig. 4). It is observed that these ranges for S_0 and L , which are compatible with neutron matter calculations (Fig. 3), are also consistent with conservative unitary gas bounds.

Conclusions: We find new bounds on the symmetry energy parameters (S_0, L) based on the conjecture that the energy of the unitary gas is less than the energy of pure neutron matter. This conjecture agrees with ab initio calculation results of pure neutron matter with NN and 3N forces. Using conservative values for the Bertsch parameter ξ , as well as the saturation properties E_0, n_0, K and K_{sym} , we find that symmetry energy parameter constraints from various nuclear experiments are consistent with the unitary gas bound. However, several theoretical interactions in active use for both theoretical calculations of dense matter and for tabulated equations of state used in astrophysical simulations of supernovae and neutron star mergers are thereby excluded. Experimental results from cold atoms having a finite scattering length [31–33] may eventually give more severe bounds, not only since $(a_0 k_F)^{-1} \simeq -0.03$ at n_0 , but also because $\xi \rightarrow 1$ for $(a_0 k_F)^{-1} \rightarrow -\infty$, i.e., $u \rightarrow 0$ (Fig. 1). Experiments imply increases of 0.03 to ξ at n_0 and 1.0 MeV to E_{UG}^0 . But p -wave and 3N interactions could also affect these values. These results will have important consequences for astrophysical simulations, as well as for predictions of radii and other structural properties of neutron stars.

ACKNOWLEDGEMENTS

This work resulted from discussions at the YIPQS long-term and Nishinomiya-Yukawa memorial workshop on Nuclear Physics, Compact Stars, and Compact Star Mergers 2016 (YITP-T-16-02). EEK, JML and IT thank the hospitality of YITP. Authors thank Stefano Gandolfi and other participants of the workshop for useful discussions, Hajime Togashi for providing numerical data, and Munekazu Horikoshi and Yoji Ohashi for inspiring suggestions. This work was supported in part by Slovak grant VEGA-1/0469/15, US DOE Grants DE-AC02-87ER40317 and DE-FG02-00ER41132, JSPS/MEXT KAKENHI Grant Nos. 15K05079, 15H03663, 16K05350, 24105001, 24105008, and NSF Grant No. PHY-1430152 (JINA Center for the Evolution of the Elements).

* e.kolomeitsev@gsi.de

† james.lattimer@stonybrook.edu

‡ ohnishi@yukawa.kyoto-u.ac.jp

§ itews@uw.edu

- [1] J.M. Lattimer and M. Prakash, *Astrophys. J.* **550**, 426 (2001).
- [2] J.M. Lattimer and M. Prakash, *Phys. Rep.* **42**, 109 (2007).
- [3] M.R. Mumpower, R. Surman, G.C. McLaughlin and A. Aprahamian, *Prog. Part. Nucl. Phys.* **86**, 86 (2016).
- [4] T. Fischer, M. Hempel, I. Sagert, Y. Suwa and J. Schaffner-Bielich, *Eur. Phys. J. A* **50**, 46 (2014).
- [5] A. Bauswein, N. Stergioulas and H.-T. Janka, *Eur. Phys. J. A* **52**, 56 (2016).
- [6] J. M. Lattimer and Y. Lim, *Astrophys. J.* **771**, 51 (2013).
- [7] M. Oertel, M. Hempel, T. Klähn and S. Typel, arXiv:1610.03361 (2016).
- [8] M. W. Zwiernik, in *Novel Superfluids vol. 2*, ed. K.-H. Bennemann and J. B. Ketterson (Oxford), Ch. 18 (2015).
- [9] M. J. H. Ku, A. T. Sommer, L. W. Cheuk and M. W. Zwiernik, *Science* **335**, 563 (2012).
- [10] G. Zürn, T. Lompe, A. N. Wenz, S. Jochim, P. S. Julienne and J. M. Hutson, *Phys. Rev. Lett.* **110**, 135301 (2013).
- [11] I. Tews, T. Krüger, K. Hebeler and A. Schwenk, *Phys. Rev. Lett.* **110**, 032504 (2013).
- [12] J. E. Lynn, I. Tews, J. Carlson, S. Gandolfi, A. Gezerlis, K. E. Schmidt and A. Schwenk, *Phys. Rev. Lett.* **116**, 062501 (2016).
- [13] K. Hebeler and A. Schwenk, *Phys. Rev. C* **82**, 014314 (2010).
- [14] H. Togashi and M. Takano, *Nucl. Phys. A* **902**, 53 (2013).
- [15] S. Gandolfi, J. Carlson and S. Reddy, *Phys. Rev. C* **85**, 032081 (2012).
- [16] A. Gezerlis and J. Carlson, *Phys. Rev. C* **81**, 025803 (2010).
- [17] A. Akmal, V. R. Pandharipande and D. G. Ravenhall, *Phys. Rev. C* **58**, 1804 (1998).
- [18] B. Friedman and V. R. Pandharipande, *Nucl. Phys. A* **361**, 502 (1981).
- [19] A. Dyhdalo, R. J. Furnstahl, K. Hebeler and I. Tews, *Phys. Rev. C* **94**, 034001 (2016).
- [20] C. Drischler, K. Hebeler and A. Schwenk, *Phys. Rev. C* **93**, 054314 (2016).
- [21] B. A. Brown and A. Schwenk, *Phys. Rev. C* **89**, 011307 (2014) Erratum: [*Phys. Rev. C* **91**, 049902 (2015)].
- [22] S. Shlomo, V. M. Kolomietz and G. Coló, *Eur. Phys. J. A* **30**, 23 (2006).
- [23] J. Piekarewicz, *J. Phys. G* **37**, 064038 (2010).
- [24] E. Khan, J. Margueron and I. Vidaña, *Phys. Rev. Lett.* **109**, 092501 (2012).
- [25] J. Margueron, private communication.
- [26] T. Klähn *et al.*, *Phys. Rev. C* **74**, 035802 (2006).
- [27] K. A. Maslov, E. E. Kolomeitsev and D. N. Voskresensky, *Nucl. Phys. A* **950**, 64 (2016).
- [28] I. Vidaña, C. Providência, A. Polls and A. Rios, *Phys. Rev. C* **80**, 045806 (2011).
- [29] C. Ducoin, J. Margueron, C. Providência and I. Vidaña, *Phys. Rev. C* **83**, 045810 (2011).
- [30] J. M. Lattimer and A. W. Steiner, *Eur. Phys. J. A* **50**, 40 (2014).
- [31] N. Navon, S. Naxcimbéne, F. Chevy and C. Salomon, *Science* **328**, 729 (2010).
- [32] H. Hu *et al.*, arXiv:1001.3200.
- [33] M. Horikoshi *et al.*, in prep.